International Journal of Rotating Machinery
2001, Vol. 7, No. 1, pp. 21–40
Reprints available directly from the publisher
Photocopying permitted by license only

Recent Development in Turbine Blade Film Cooling*

JE-CHIN HAN† and SRINATH EKKAD‡

Turbine Heat Transfer Laboratory, Mechanical Engineering Department, Texas A&M University, College Station, TX 77843-3123, USA

(Received in final form 10 March 1999)

Gas turbines are extensively used for aircraft propulsion, land-based power generation, and industrial applications. Thermal efficiency and power output of gas turbines increase with increasing turbine rotor inlet temperature (RIT). The current RIT level in advanced gas turbines is far above the melting point of the blade material. Therefore, along with high temperature material development, a sophisticated cooling scheme must be developed for continuous safe operation of gas turbines with high performance. Gas turbine blades are cooled internally and externally. This paper focuses on external blade cooling or so-called film cooling. In film cooling, relatively cool air is injected from the inside of the blade to the outside surface which forms a protective layer between the blade surface and hot gas streams. Performance of film cooling primarily depends on the coolant to mainstream pressure ratio, temperature ratio, and film hole location and geometry under representative engine flow conditions. In the past number of years there has been considerable progress in turbine film cooling research and this paper is limited to review a few selected publications to reflect recent development in turbine blade film cooling.

Keywords: Gas turbine, Film cooling, Heat transfer

INTRODUCTION

Advanced gas turbine engines operate at high temperatures (1200–1400°C) to improve thermal efficiency and power output. As the turbine inlet temperature increases, the heat transferred to the blades in the turbine also increases. The level and variation in the temperature within the blade material (which causes thermal stresses) must be limited to achieve reasonable durability goals. Also the temperatures are far above the permissible metal temperatures due to which there is a need to cool the blades to operate without failure. The blades are cooled by extracted air from the compressor of the engine. Since this extraction incurs a penalty to the thermal efficiency, it is necessary to understand and optimize the cooling for the engine, turbine operating conditions, and turbine blade geometry.

* This paper was presented at the 11th International Symposium on Transport Phenomena.

† Corresponding author. Tel.: 409 845-3738. Fax: 409 862-2418. E-mail: jchan@mengr.tamu.edu.
‡ Present address: Assistant Professor, Mechanical Engineering Department, Louisiana State University, Baton Rouge, LA 70803, USA.

Gas turbine blades are cooled internally and externally. Internal cooling is achieved by passing the coolant through several enhanced serpentine passages inside the blades and extracting the heat from the outside of the blades. Jet impingement cooling and pin fin cooling are also utilized as a method of internal cooling. External cooling is also called film cooling. Internal coolant air is ejected out through discrete holes or slots to provide a coolant film to protect the outside surface of the blade from hot combustion gases.

Fundamentals of Film Cooling

Film cooling primarily depends on the coolant-to-hot mainstream pressure ratio (p_c/p_t), temperature ratio (T_c/T_g), and the film cooling hole location, configuration and distribution on a film cooled airfoil. The coolant-to-mainstream pressure ratio can be related to the coolant-to-mainstream mass flux ratio (blowing ratio) while the coolant-to-mainstream temperature ratio can be related to the coolant-to-mainstream density ratio. In a typical gas turbine airfoil, the p_c/p_t ratios vary from 1.02 to 1.10, corresponding blowing ratios approximately from 0.5 to 2.0, while the T_c/T_g values vary from 0.5 to 0.85, corresponding density ratios approximately from 2.0 to 1.5. Both pressure ratio (p_c/p_t), and temperature ratio (T_c/T_g), are probably the most useful measure in quantifying film cooling effectiveness since these ratios essentially gives the ratio of the coolant to hot mainstream thermal capacitance. In general, higher the pressure ratio, better the film cooling protection (i.e., reduced heat transfer to the airfoil) at a given temperature ratio, while lower the temperature ratio, better the film cooling protection at a given pressure ratio. However, too high of pressure ratio (i.e., blowing too much) may reduce the film cooling protection, because of jet penetration into the mainstream (jet lift-off from the surface). Therefore, it is important to optimize the amount of coolant for airfoil film cooling under engine operating conditions (Reynolds number $\sim 10^6$, Mach number ≈ 0.9 at exit conditions). For designing a better film cooling pattern of an airfoil, turbine cooling system designers also need to know where heat is transferred from hot mainstream to the airfoil. As mentioned earlier, these film-hole pattern (i.e., film hole location, distribution, angle and shape) would affect film cooling performance. There are many film cooling papers available in the open literature. This paper is limited to review a few selected papers to reflect recent development in turbine blade film cooling. Specifically, this review focuses on the following topics: rotor blade film cooling, nozzle guide vane film cooling, airfoil endwall film cooling, as well as airfoil leading edge and blade tip region film cooling. Several papers for rotator blade, stator vane, and endwall film cooling, under representative engine flow conditions, are reviewed and discussed. Some parametric studies for large-scale cascade blade, cascade vane, cascade endwall, simulated blade tips and leading edge region film cooling under low speed flow conditions are also reviewed and discussed.

Figure 1 shows the schematic of film cooling concept. Typically, the heat load to the surface without film cooling is represented as heat flux $q_0'' = h_0(T_g - T_w)$, where h_0 is the heat transfer coefficient on the surface with wall temperature T_w and oncoming gas temperature (T_g). When coolant is injected on the surface, the driving temperature is T_f, film temperature, which is a mixture of gas (T_g) and coolant temperature (T_c), $q'' = h(T_f - T_w)$, where h is the heat transfer coefficient on the surface with film injection. Also, a new term film effectiveness (η) is introduced, where $\eta = (T_g - T_f)/(T_g - T_c)$. The η values vary between 0 and 1 with

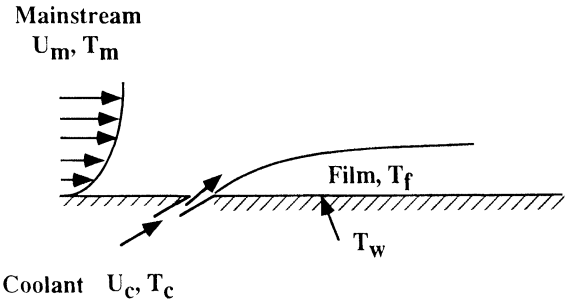

FIGURE 1 Schematic of film cooling concept.

1 as the best film cooling effectiveness. Therefore, the heat flux ratio can be written as: $q''/q_0'' = (h/h_0)[(T_f - T_w)/(T_g - T_w)] = (h/h_0) \times [1 - \eta(T_g - T_c)/(T_g - T_w)]$. To obtain any benefit from film cooling, the heat load ratio, q''/q_0'', should be below 1.0. The heat transfer coefficient ratio (h/h_0) is enhanced due to turbulent mixing of the jets with the mainstream and is normally greater than 1.0. The temperature ratio $(T_f - T_w)/(T_g - T_w)$, which is related to the film effectiveness should be much lower than 1.0 such that the heat load ratio is lower than 1.0. The best film cooling design is to reduce the heat load ratio (i.e., smaller h/h_0 enhancement with greater η) for a minimum amount of coolant available for a film cooled airfoil.

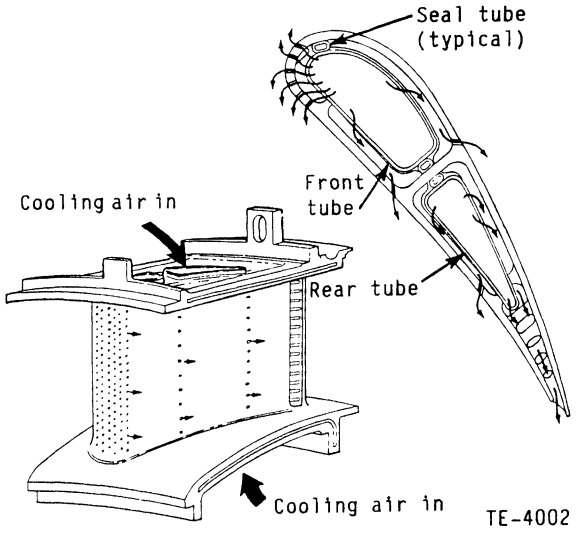

FIGURE 2 Typical cooled airfoil (Nirmalan and Hylton, 1990).

FILM COOLING ON NOZZLE GUIDE VANES

It is well known that nozzle guide vanes being just downstream of the combustor exit, experience the hottest gas path temperatures. The vanes also experience high free-stream turbulence caused by combustor mixing flows. Depending on the requirements, vanes are cooled internally and some coolant is ejected out as film cooling. It is important to understand the effects of high free-stream turbulence on vane surface heat transfer. Since vanes operate at the highest temperatures in the turbine section, it is imperative that there is a need for adequate and efficient cooling system to ensure that vanes survive for their estimated life. A typical film cooled vane is shown in Fig. 2. The vane has an internal impingement tube through which the coolant enters the core of the vane and then impinges on the inside surface of the outer wall. The coolant is ejected out of discrete film hole rows at various axial locations on the airfoil.

Hot Cascade NGV Film Cooling

Nirmalan and Hylton (1990) studied the effects of film cooling on a turbine vane in a aerothermodynamic cascade. They maintained conditions similar to ranges existing in real engines. They performed experiments on a three-vane hot cascade and studied the effects of parameters such as Mach number, Reynolds number, coolant-to-gas temperature ratio, and coolant-to-gas pressure ratio. The C3X vane film cooling geometry consists of hole arrays on the leading edge, the suction surface, and the pressure surface. The leading edge has a showerhead array of five equally spaced rows with the central row located at the aerodynamic stagnation point. Two rows each on the pressure and suction surfaces are located downstream. The hole rows are also staggered with holes in the second row located midway between the holes in the first row. More details on the film hole geometry are given in the paper. Typical results are presented for a cascade exit Mach number of 0.9 and exit Reynolds number of 2.0×10^6.

The results in this paper are presented in the form of Stanton number reduction (SNR) which is mainly to isolate the differences between non-film cooled and film cooled heat transfer. The SNR is defined as $\text{SNR} = 1 - (\text{St}_{\text{FC}}/\text{St}_{\text{NFC}})$. When SNR is greater or less than zero, it implies reduced or increased heat transfer levels for film cooled airfoil over an uncooled airfoil. Figure 3 shows the

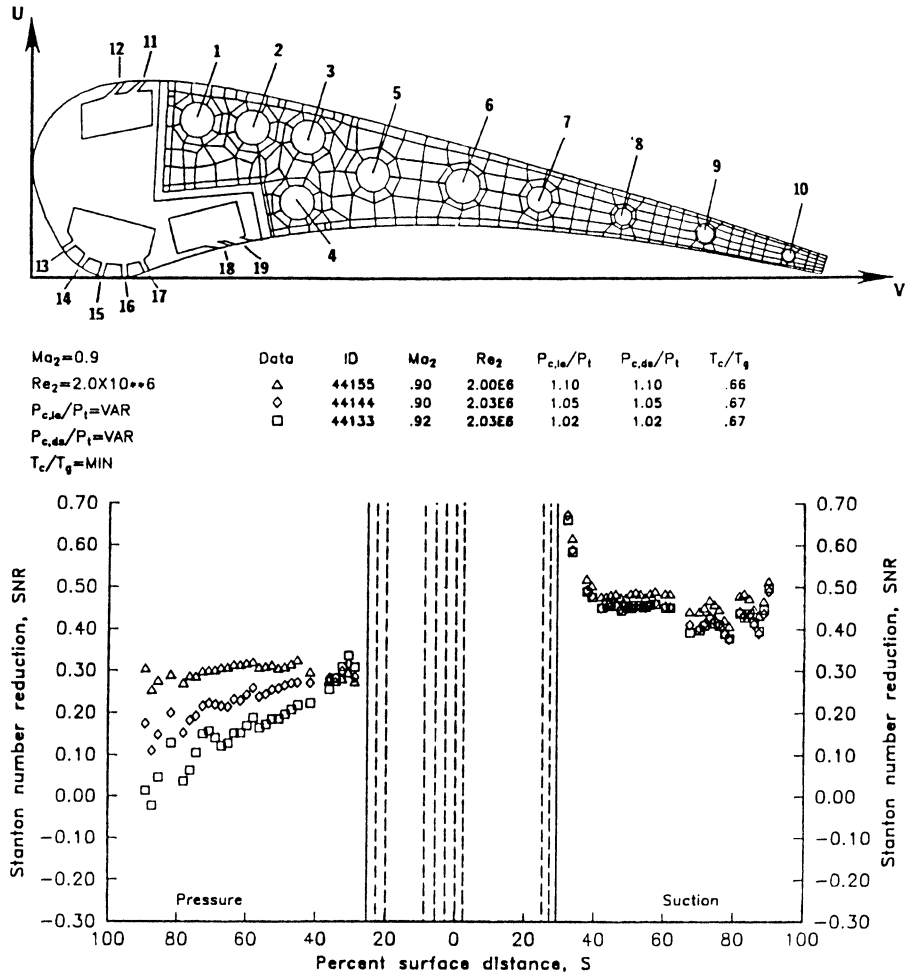

FIGURE 3 Effects of leading edge and downstream blowing on Stanton number reduction (Nirmalan and Hylton, 1990).

effects of varying blowing strength (coolant-to-gas pressure ratio, p_c/p_t) at two thermal dilution levels (coolant-to-gas temperature ratio, T_c/T_g). For the case of lower $T_c/T_g = \text{MIN}$ (~ 0.67), the SNR values on most part of the suction side are around 40% while these values on the pressure side can be up to 30% near the trailing edge depending on the coolant-to-gas pressure ratio. A positive SNR value is seen on both surfaces with film cooling. However, the effect of blowing strength is evident on the pressure surface only. With increasing blowing strength, the effect on the pressure surface increases farther downstream. However, suction surface shows little effect of blowing strength. This is explained with the reason that the film coolant flow on the suction surface to be choked over this range of pressure ratios ($p_c/p_t = 1.02$–1.05) which makes the effect of blowing invariant. For the case of higher $T_c/T_g = \text{MAX}$ (~ 0.85), the effects are similar as that for lower $T_c/T_g = 0.67$. However, the effect of blowing strength on the pressure surface is reduced and the levels of SNR values are lower on both surfaces. The SNR values on most part of the suction side are about 20% while these values on the pressure side are only about 10% depending on the blowing strength. This happens because, for higher $T_c/T_g = 0.85$, the temperature difference between the coolant and the

gas is smaller, thus the film cooling effect is reduced. This study also indicate (not shown here) that, at lower coolant-to-gas temperature ratio ($T_c/T_g \sim 0.67$), the film cooling effects are relatively insensitive to exit Mach numbers; and higher favorable film cooling effects are seen at higher exit Reynolds numbers. On the other hand, at high coolant-to-gas temperature ratio ($T_c/T_g \sim 0.85$), film cooling effects are dependent on exit Mach number, and lesser effects due to exit Reynolds number are seen. Another hot cascade nozzle guide vanes (NGV) film cooling study could be referred to Abuaf *et al.* (1995). They used a warm (315°C) wind tunnel test facility equipped with a linear cascade of film cooled vane airfoils for simultaneous determination of the local heat transfer coefficients and the adiabatic film cooling effectiveness.

Cascade Vane Film Cooling

Ames (1997) studied a similar C3X vane with film cooling in a four-vane ambient cascade. The influence of high free-stream turbulence on vane heat transfer coefficient and film effectiveness distributions was reported. A high level, large-scale inlet turbulence was generated with a mock combustor (Tu = 12%) and was used to contrast results with a low level (Tu = 1%) of inlet turbulence. For the heat transfer tests, the coolant temperature was kept the same as the mainstream ambient temperature. For the film effectiveness tests, the coolant temperature was heated slightly higher than the mainstream air temperature which produced a coolant to mainstream density ratio (DR) = 0.95. Figure 4 shows the effect of free-stream turbulence on adiabatic film effectiveness ratio distributions for the case of film cooling on the blade pressure surface, and on the showerhead region respectively, under different velocity ratio. The adiabatic film effectiveness ratio is the adiabatic film effectiveness with high inlet turbulence (Tu = 12%) divided by that with low inlet turbulence (Tu = 1%). Lower value of the ratio implies lower film cooling effectiveness due to free-stream turbulence effect. Turbulence was found to have a dramatic influence on pressure surface film cooling effectiveness, particularly at the lower velocity ratios. Turbulence was found to substantially reduce film cooling effectiveness levels produced by showerhead film cooling.

They also studied the effect of coolant to mainstream velocity ratio (Vr) on Stanton number ratio distributions for film injection on the blade suction and pressure sides, respectively under high inlet turbulence condition (Tu = 12%). The Stanton number ratio is the heat transfer coefficient with film injection divided by that without film injection. Higher values of the ratio implies higher heat transfer augmentation due to film injection. Film injection was found to have only a moderate heat transfer augmentation (up to 20%) on the downstream from arrays on the suction surface where the boundary layer was turbulent (not shown here). However, film injection was found to have a substantial heat transfer augmentation (up to 100%) on the downstream from the arrays on the pressure surface where the boundary layer was laminar. In general, heat transfer augmentation was found to scale on velocity ratio.

Another ambient cascade vane film cooling was done by Drost and Bölcs (1998). They used a transient liquid crystal technique for measuring detailed heat transfer coefficient and film effectiveness distributions on a turbine NGV airfoil in a five vane linear cascade at two mainstream turbulence intensities of 5.5% and 10%. They found that mainstream had only a weak influence on suction surface film cooling. Higher film effectiveness was noted on the pressure surface at high turbulence due to increased lateral spreading of the coolant.

FILM COOLING ON ROTOR BLADES

Rotating Blade Film Cooling

The designers expect to see actual heat transfer data under real experimental conditions. But, it is very difficult to obtain results under real engine condition experiments. However, there are very few results on real rotating blades. Abhari and Epstein (1994) presented time-resolved measurements of

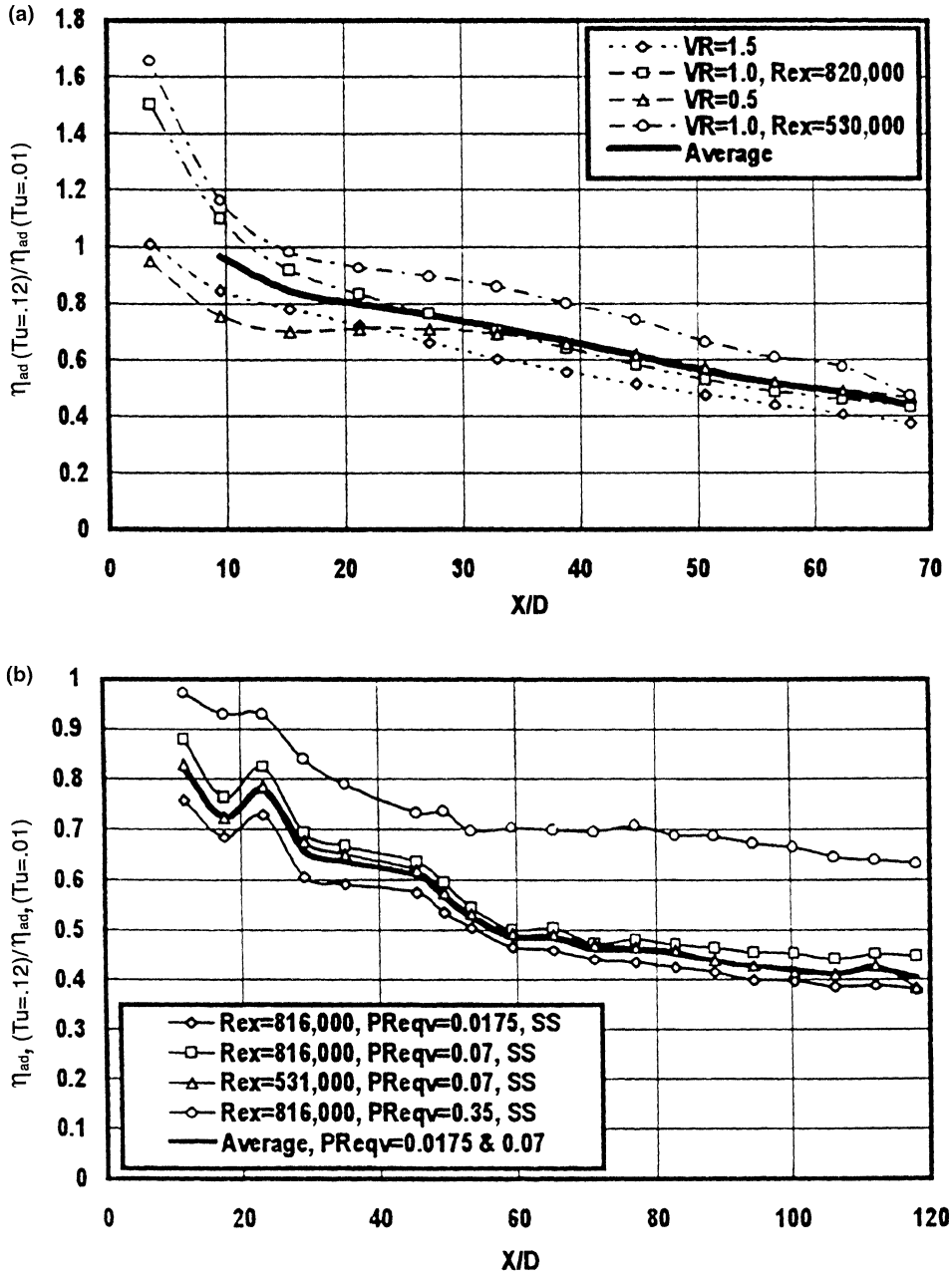

FIGURE 4 (a) Influence of turbulence on relative level of pressure surface adiabatic effectiveness, two rows, 30° holes, DR = 0.94, $p/d = 3.0$ (Ames, 1997). (b) Influence of turbulence on relative level of suction surface adiabatic effectiveness for showerhead array, DR = 0.94 (Ames, 1997).

heat transfer on a fully cooled transonic turbine stage. They conducted experiments in a short duration blow down turbine test facility at MIT, which simulated full engine scale Reynolds number, Mach number, Prandtl number, gas to wall, and coolant-to-mainstream temperature ratios, specific heat and flow geometry. They used Freon-12 in the mainstream and used Argon/Freon-14 mixture for

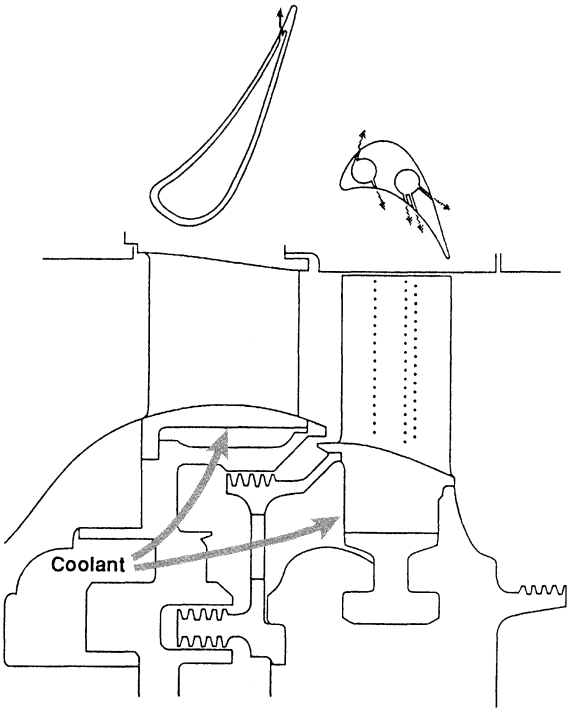

FIGURE 5 Turbine geometry and cooling arrangement (Abhari and Epstein, 1994).

the coolant. The turbine geometry and cooling arrangements are shown in Fig. 5. More details on the blade geometry can be obtained from Abhari and Epstein (1994).

Figure 6 presents the time resolved rotor blade heat transfer measurements for cooled and uncooled rotor blades. For the case of film cooled blade, the coolant-to-gas temperature ratio (T_c/T_g) is about 0.51 while the coolant blowing ratio is about 1.24 and 1.52 on the first row of suction surface and pressure surface, respectively. Over the pressure surface, film injection has a little effect on heat transfer levels. Comparing the midspan levels for uncooled and cooled rotors, film injection has a strong effect over the entire suction surface. Film injection produces a strong reduction in heat transfer levels on the suction surface (up to 60%) and a small effect on the pressure surface. Film injection, thus can produce a significant reduction in heat load to the blade from the hot mainstream gases. The significant reductions indicate the strong advantages of a film cooling scheme. At the crown of the suction surface (Fig. 6(a)), the film cooling is prominent at midspan but minimal at the hub. Elsewhere on the suction surface, the film cooling is similar at midspan and hub. It is seen that film cooling is to reduce the heat transfer and also to introduce a phase shift in the unsteady waveform. This unsteady heat transfer might be due to the potential interactions between blade rows and impingement of the NGV wakes and shock waves on the rotor blade.

Another rotating blade film cooling study could be found from Takeishi *et al.* (1992). They used heat and mass transfer analogy technique for measuring film cooling effectiveness on a rotating blade test facility. They concluded that the film cooling effectiveness on the suction surface of the rotating blade compares well with that on the stationary blade cascade, but a low level of effectiveness appears on the pressure surface of the rotating blade.

Cascade Blade Film Cooling

Most experimental results for turbine blades are obtained on simulated cascades under simulated engine conditions. Several studies have focused on turbine blade film cooling by simulating real engine conditions in ambient cascades. Camci and Arts (1985a,b; 1990) undertook a series of work at the Von Karman Institute of Fluid dynamics (VKI) on high pressure rotor blade heat transfer measurements. Rotor blades were tested under simulated conditions in a stationary mode using platinum thin film gauges painted on a blade made of machinable glass ceramic. They tested for a blade with leading edge film cooling array and the other blade with suction side two-row film cooling. The film cooling hole geometry is very important in discussing the effect of film injection on heat transfer levels. They measured local heat flux using thin film gauges for blades with and without film cooling holes. The VKI isentropic compression tube facility generated mainstream pressure and temperature close to 3 bar and 410 K, respectively. The coolant-to-mainstream temperature ratio (T_c/T_∞) was

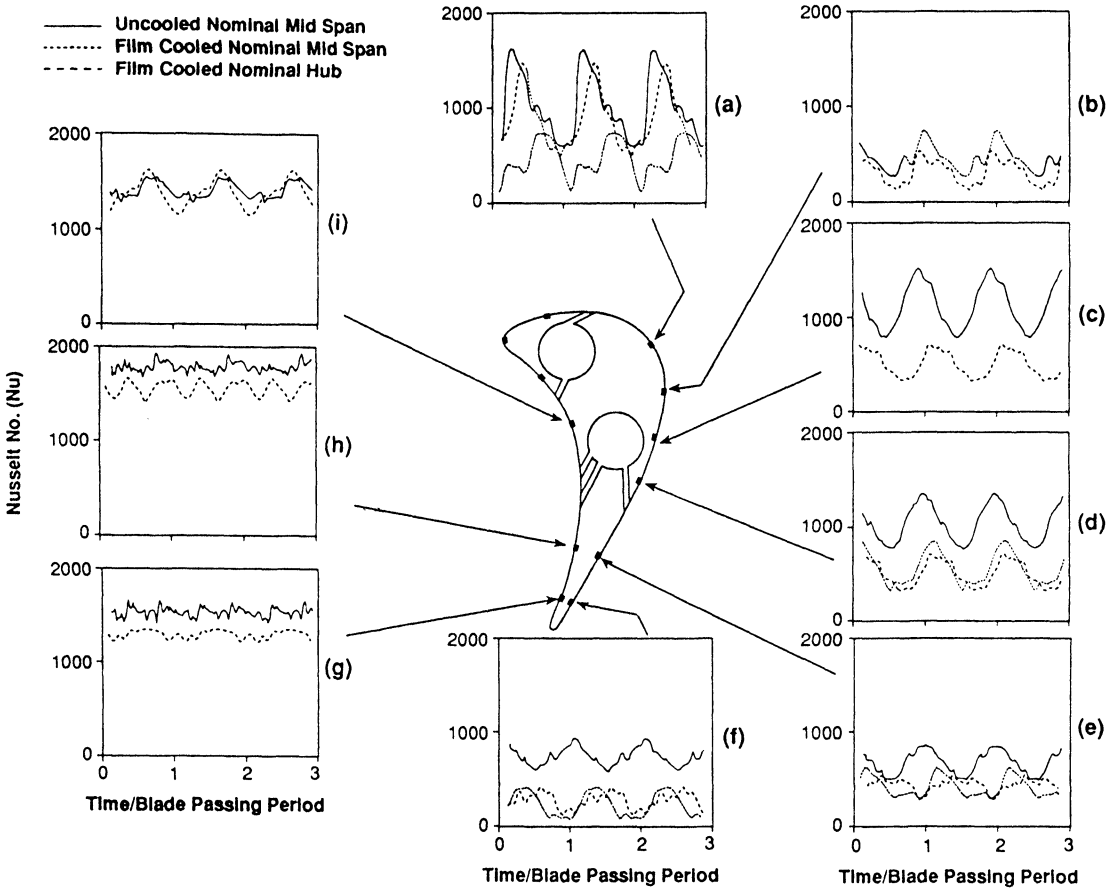

FIGURE 6 Time-resolved rotor heat transfer measurements compared with those for an uncooled rotor (Abhari and Epstein, 1994).

varied from 0.4 to 0.7. Coolant to mainstream mass flux ratio (m_c/m_∞) was also varied from 0.48 to 1.01.

Figure 7 presents the data for a blade with leading edge film holes. Heat transfer distributions for $m_c/m_\infty = 0.6\%$ and $T_c/T_\infty = 0.52$ and 0.59. The effect of introducing film cooling is the lowering of heat transfer into the turbine blade compared to the levels obtained on the blade without film holes. The effect of film cooling in reducing heat transfer levels is strongly evident in the figure. Heat transfer levels increase gradually downstream and reach uncooled levels close to trailing edge. The cooling efficiency increases with decreasing T_c/T_∞ which is as expected. When cooler flow is injected, the blade receives more protection downstream of injection. In that case, lower heat transfer levels are expected. Figure 8 presents the effect of suction side film cooling on heat transfer for different T_c/T_∞ levels at two different coolant blowing rates. Significant heat transfer reductions are observed in the region for $X/d < 40$ for both blowing ratios of 0.4 and 0.96. Further downstream, the effects are reduced and the heat transfer levels approach uncooled levels. However, the film cooling effect is still significant at $X/d = 100$ for $M = 0.96$. Also the effect of temperature ratio is also stronger at higher blowing ratio. The results indicate that at low blowing ratios, the effect of temperature ratio is smaller compared to that for $M = 0.96$ (not shown here).

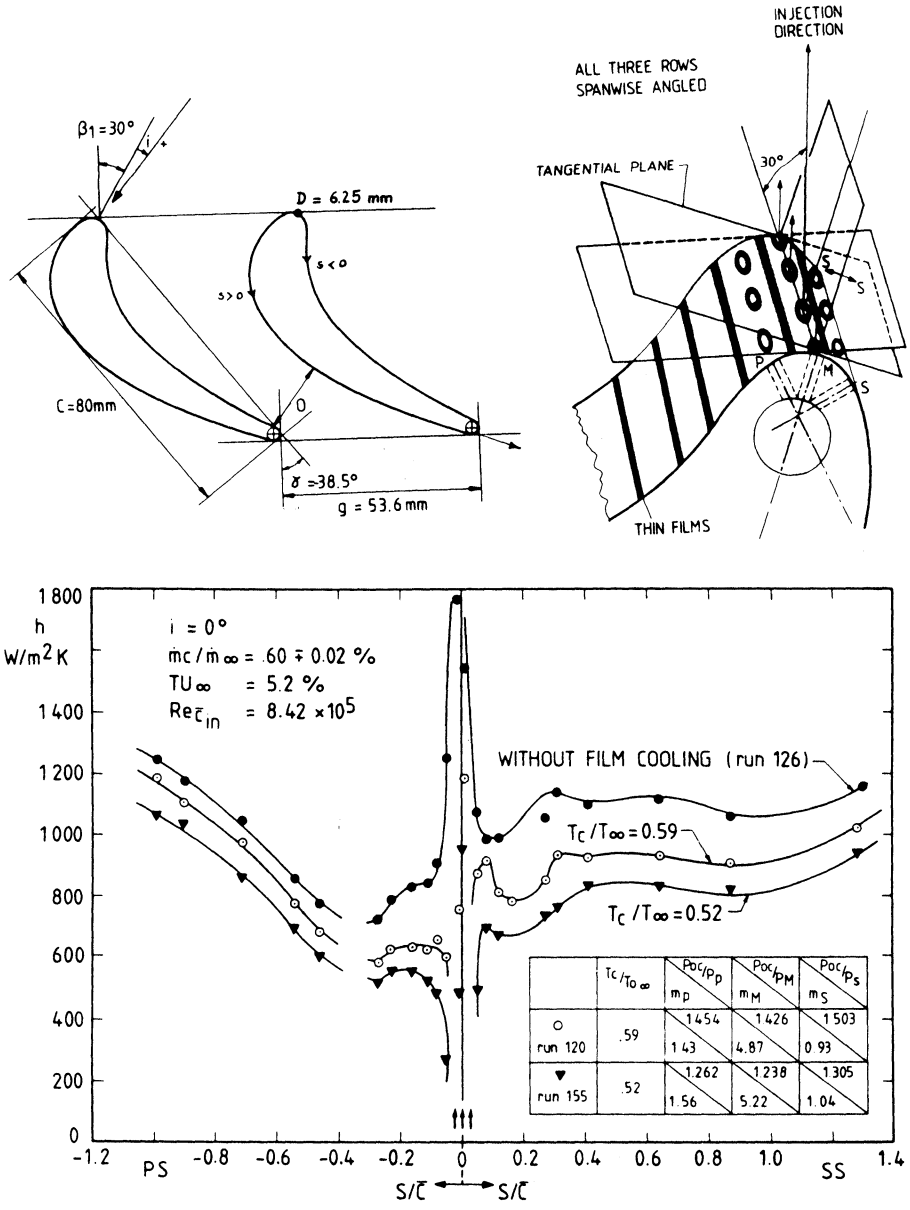

FIGURE 7 Leading edge heat transfer with film cooling (Camci and Arts, 1985a).

Unsteady Wake Effect on Cascade Blade Film Cooling

It is well known that downstream turbine blades are affected by unsteady wakes shed by upstream vane trailing edges. Wake simulation experiments focus on the effects of unsteady wakes on downstream film cooled turbine blades. The film cooled blades are stationary and upstream rotating rods simulate the unsteady wakes. Ou *et al.* (1994) and Mehendale *et al.* (1994) at Texas A&M University used the spoked wheel type wake generator as shown in Fig. 9 to simulate the effect of unsteady wake on downstream blade film cooling performance.

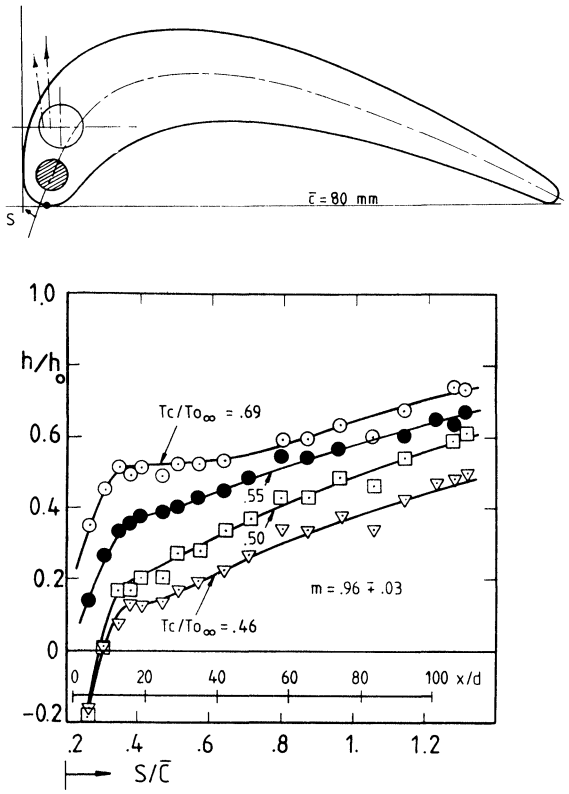

FIGURE 8 Suction side heat transfer with film cooling, effect of temperature ratio (Camci and Arts, 1985b).

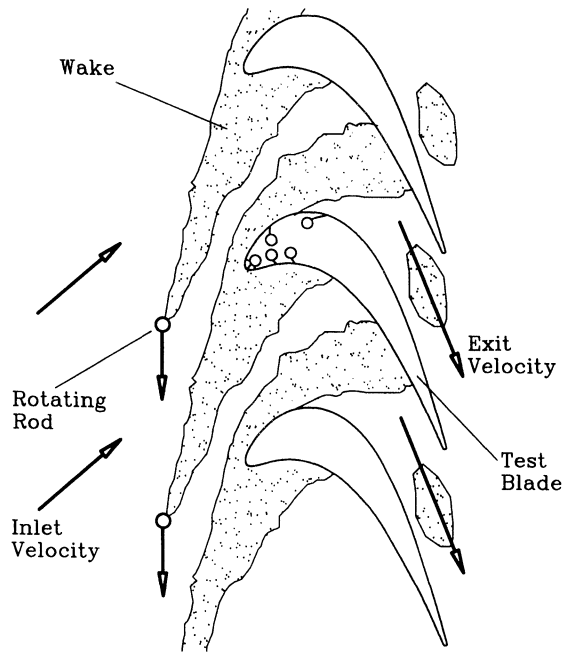

FIGURE 9 Conceptual view of unsteady wake effect on a model blade with film holes.

A typical advanced high pressure turbine blade was chosen for this study in a large-scale low speed linear 2-D turbine cascade facility. The selected blade has three rows of film cooling holes on the leading edge and two rows each on the pressure and suction surfaces. The unsteady wake strength could be represented by a wake Strouhal number. Wake Strouhal numbers ($S=2\pi Ndn/60V_1$) were simulated to be consistent with real engine values ($S=0.05$–0.3), wake generator speed (N), wake rod diameter (d), number of rod (n), and upstream mainstream velocity (V_1) could be varied to generate a range of Strouhal number. Air and CO_2 were used as coolant to simulate different coolant-to-mainstream density ratio effect. Coolant blowing ratio (M) was varied from 0.4 to 1.2. For the heat transfer tests, the coolant temperature was kept the same as the mainstream ambient temperature, the coolant-to-mainstream DR was 1.0 and 1.52 respectively for air and CO_2 as coolant. For the film cooling tests, the coolant was heated slightly higher than the mainstream temperature, the density ratio was 0.97 for air and 1.4 for CO_2 as coolant. Du *et al.* (1997) used a transient liquid crystal technique to measure the detailed heat transfer coefficient and film cooling effectiveness distributions on the same film cooled blade from the same unsteady wake facility. They concluded that Nusselt numbers for a film cooled blade are much higher compared to a blade without film injection, as shown in Fig. 10. Particularly, film injection causes earlier boundary layer transition on the suction surface. Unsteady wakes slightly enhance Nusselt numbers but significantly reduce film cooling effectiveness on a film cooled blade compared with a film cooled blades without wakes. Nusselt numbers increase slightly but film cooling effectiveness increases significantly with an increase in film cooling blowing ratio for CO_2 injection. Higher density coolant (CO_2) provides higher effectiveness at higher blowing ratios

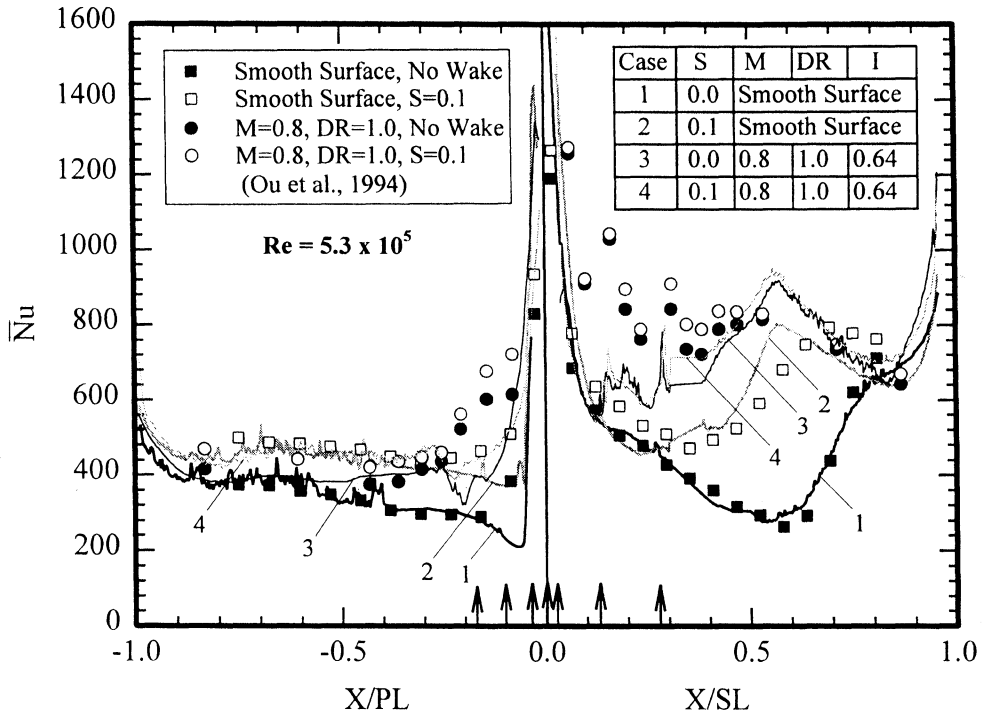

FIGURE 10 Effect of unsteady wake on spanwise-averaged Nusselt number distributions for air injection (cases 1–4), $M = 0.8$ (Du *et al.*, 1997).

($M = 1.2$) whereas lower density coolant (Air) provides higher effectiveness at lower blowing ratios ($M = 0.8$). Figure 11 shows the effect of a moderate unsteady wake ($S = 0.1$, case 4) on detailed film cooling effectiveness distributions for air as coolant at $M = 0.8$. Without unsteady wake (case 3), the film cooling jets protect the surface better with limited mixing with the mainstream. Addition of unsteady wakes (case 4) causes disturbances in the mainstream which result in more mixing between the mainstream and coolant jets and reduce protection of the surface by the coolant jets.

FILM COOLING ON AIRFOIL ENWALLS

Endwall film cooling has gained significant importance due to the usage of low aspect ratio and low solidity turbine designs. Film cooling and associated heat transfer is strongly influenced by the secondary flow effects. Figure 12 shows the conceptual view of the 3-D flow field inside the endwall region (Goldstein and Spores, 1988). The location of film holes and their cooling effectiveness is strongly influenced by the presence of these secondary flows. Locating film cooling holes on endwall requires complete understanding of secondary flow behavior and associated heat transfer. To that end, heat transfer researchers have focused on several film cooling configurations for endwall film cooling.

Annular Cascade NGV Endwall Film Cooling

Harasgama and Burton (1991a,b) reported the heat transfer measurements on the endwalls of a short duration annular cascade of turbine NGV in the presence of film cooling. Based on the predicted Mach number contours on the outer endwall, they proposed to place a row of inclined film cooling holes along an iso-Mach line ($M = 0.25$), thus ensuring a uniform blowing rate and momentum flux

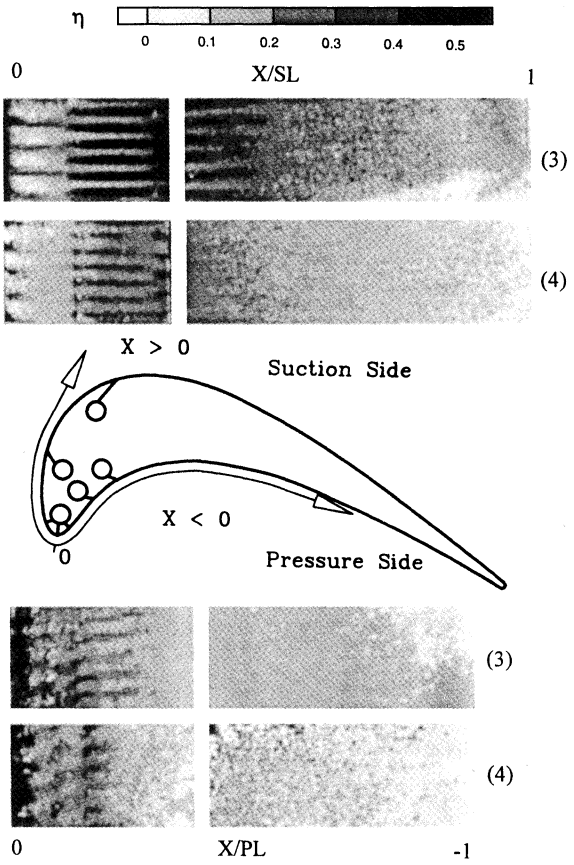

FIGURE 11 Effect of unsteady wake on detailed film cooling effectiveness distributions for air injection (cases 3–4), $M = 0.8$ (Du *et al.*, 1997).

ratio as the coolant emerges into the mainstream. The NGV were tested at the correct engine non-dimensional conditions of Reynolds number ($= 2.55 \times 10^6$ based on exit conditions), Mach number ($= 0.93$ based on exit conditions), gas-to-wall temperature ratio ($= 1.3$), and coolant-to-gas density ratio ($= 1.80$). Figure 13 shows the ratio of cooled-to-uncooled Nusselt number for a typical NGV operating conditions ($G =$ blowing ratio $= 1.11$, $\theta = (T_g - T_c)/(T_g - T_w) =$ gas-to-coolant temperature difference ratio $= 1.44$). The results indicated that the secondary flow and horseshoe vortex interact with the coolant jet which is converted towards the suction side of the NGV endwall passage. Therefore, the coolant does not quite reach the pressure side trailing edge, leading to diminished cooling in this region. It is clear that over most of the endwall the heat transfer is reduced by 50–70%, except near the pressure side trailing edge corner where the reduction is about 20%.

Another annular cascade NGV endwall film cooling study was done by Takeishi *et al.* (1990). They used thin foil heaters with thermocouples for measuring heat transfer and film cooling effectiveness on the endwall of an airfoil in a low speed, fully annular, low aspect ratio vane cascade. They concluded that the secondary flow could significantly modify the cooling effectiveness distributions on the endwall. The coolant was convected towards the suction side of the endwall leaving the pressure side trailing edge region relatively unprotected.

Linear Cascade Blade Endwall Film Cooling

Friedrichs *et al.* (1996) reported the distribution of adiabatic film cooling effectiveness on the endwall of a large-scale low-speed linear turbine blade cascade using the ammonia and diazo coating surface technique. Prior to the experiment, diazo coated paper or diazo film is fixed to the test surface. The cooling air is seeded with ammonia gas and water vapor. During the film injection experiment, the ammonia gas reacts with the diazo coating, leaving traces of varying darkness over the test surface. The darkness of the traces of the diazo surface coating is dependent on the surface concentration of the ammonia and water vapor in the coolant gas. They developed a calibration curve between the darkness and relative concentration using an optical scanner, therefore, the adiabatic film cooling effectiveness could be quantified using the principle of heat and mass transfer analogy. Figure 14 shows the endwall film cooling effectiveness distributions, which were processed from those traces on the surface coating of the turbine endwall. The results reveal the strong interactions between endwall coolant injection and secondary flows in the blade passage. Coolant injection underneath the lift-off lines is inefficient,

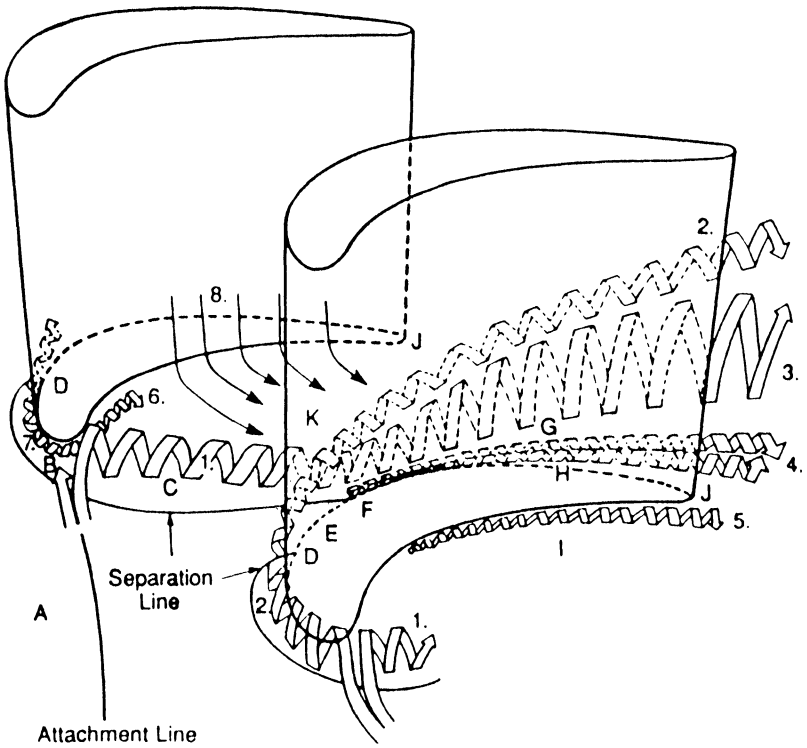

1. Leading edge pressure side vortex
2. Leading edge suction side vortex
3. Passage vortex
4. Suction side corner vortices
5. Pressure side corner vortex
6. Pressure side leading edge corner vortex
7. Suction side leading edge corner vortex
8. Downward velocity component on pressure side

FIGURE 12 The three-dimensional flow field in the endwall region (Goldstein and Spores, 1988).

as most of the coolant leaves the surface. Coolant injection away from the lift-off lines can provide a larger cooling area. In general, the coolant jet traces do not follow the injection angle, except near the film cooling holes. The area averaged cooling effectiveness was about 12.3%. The cooling holes distributions could be re-arranged in order to provide a better film cooling coverage (Friedrichs *et al.*, 1998).

Another linear cascade blade endwall film cooling study could be referred to (Jabbari *et al.*, 1994). They used ammonia-diazo-paper for visualizing of the coolant jet traces and heat-mass transfer analogy for determining the film effectiveness distributions on the endwall of a turbine blade in a low-speed, large-scale linear blade cascade. Their tests included three blowing ratios, two density ratios, and two Reynolds numbers.

TURBINE BLADE TIP FILM COOLING SIMULATION

Perhaps late Dr. D.E. Metzger did the most comprehensive study on blade tip film cooling at Arizona State University. The blade tip is the most critical area of a turbine engine. The tip region lacks durability and is difficult to cool. The clearance leakage flow across the tip from the pressure side to suction side causes the blade tip failure. Figure 15 shows the clearance gap leakage flow and blade tip film configurations that are used in modern

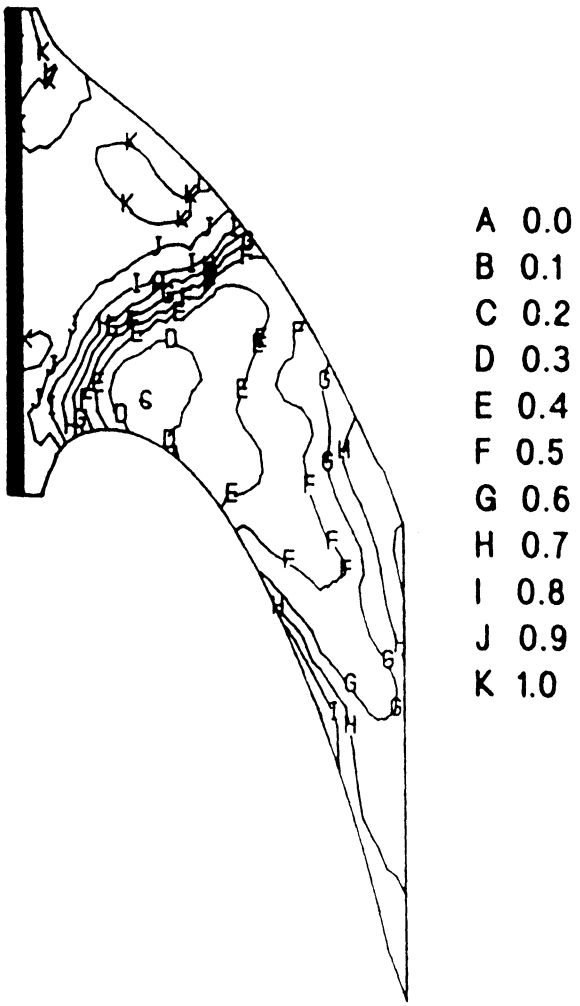

FIGURE 13 Ratio of cooled to uncooled Nusselt number for $G = 1.11$, $\theta = 1.44$ (Harasgama and Burton, 1991a).

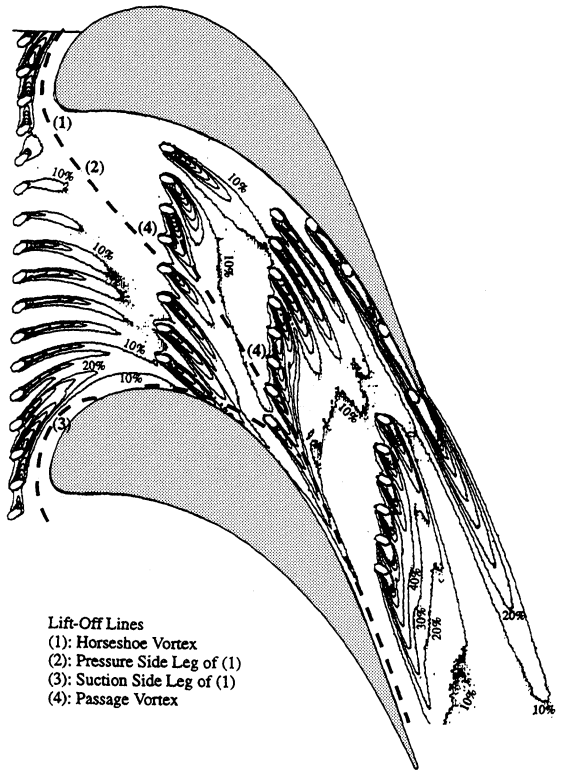

FIGURE 14 Adiabatic film cooling effectiveness on the end-wall surface for the datum cooling configuration, at an inlet blowing ratio of $M_{\text{inlet}} = 1.0$ (Friedrichs *et al.*, 1996).

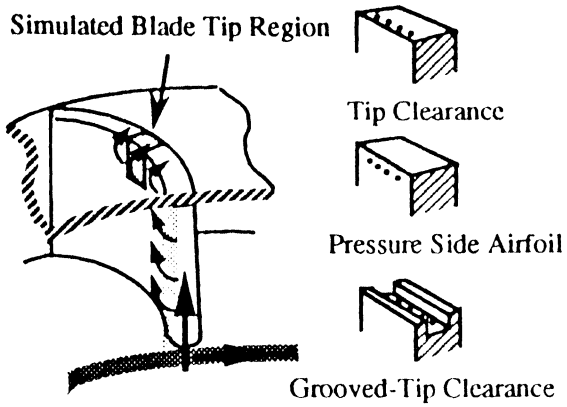

FIGURE 15 Clearance gap leakage and blade tip film cooling configurations (Kim *et al.*, 1995).

engines. A summary of cooled tip heat transfer investigations of Dr. Metzger was published a few years ago (Kim *et al.*, 1995). This study presents a comparison of various tip cooling configurations and their effects on film effectiveness and heat transfer coefficient using a transient liquid crystal technique.

Figure 16 shows the character of the clearance gap flow and blade tip geometry and film injection configurations studied by Metzger *et al.* A forced flow through a thin clearance gap (H) was used to simulate the blade tip leakage flow. A film cooling loop provided the coolant flow for the experiments. Four film cooling configurations were tested: (a) discrete slot injection, (b) round hole injection, (c) pressure side flared hole injection, and

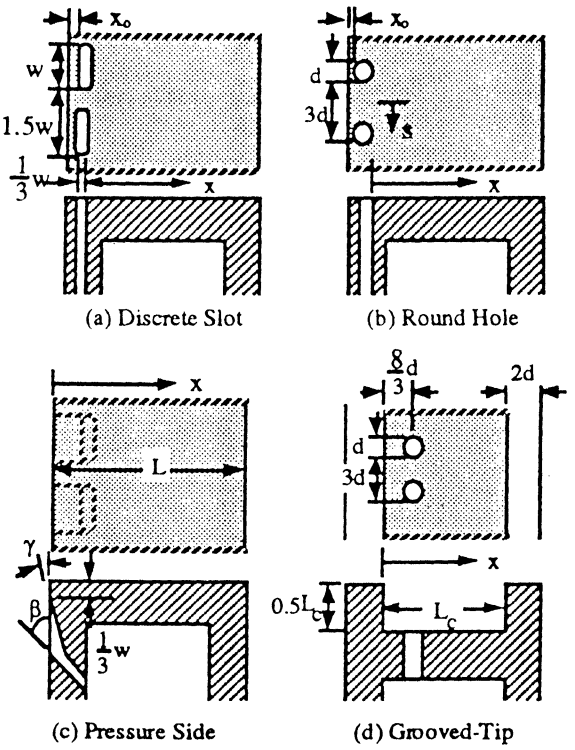

FIGURE 16 Blade tip geometry and film injection configurations (Kim *et al.*, 1995).

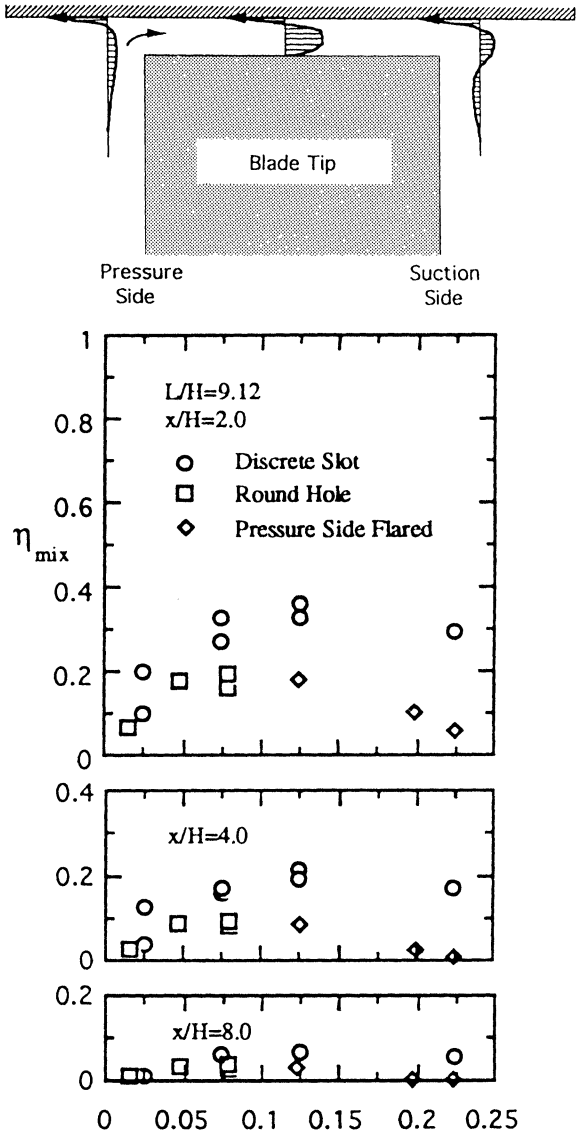

FIGURE 17 Film cooling performance comparisons using mixed mean correlation (Kim *et al.*, 1995).

(d) grooved tip cavity injection. Figure 17 present the effect of coolant-to-mainstream mass flow rate ratio (R) on cross-stream averaged film cooling effectiveness for this four film cooling configurations. For the discrete slot injection, film effectiveness decreases from the injection location but increases with increasing coolant-to-mainstream mass flow rate ratio. For the round hole injection, film effectiveness initially increases with mass flow rate then reaches a constant level at higher mass flow rate ratio. However, for the pressure side flared hole injection, film effectiveness is insensitive to the two mass flow rate ratios shown here. Film effectiveness data for the round hole injection are about the same as the flared injection, but are lower than the slot injection. For the case of grooved tip cavity injection, the trend shows that suction side injection inside the grooved tip cavity produces higher film effectiveness than the pressure side injection. It may be due to the cavity flow effect when the coolant is pushed on to the tip surface by the recirculating leakage flow inside the cavity. It is noted that the typical pressure driven flow across the tip is more complex than the simple leakage flow modeled by the above study. More real leakage flow studies with film cooling heat transfer measurements are needed for improving blade tip film cooling design.

LEADING EDGE REGION FILM COOLING SIMULATION

Film cooling around the turbine leading edge region not only protects the region from hot gases but also affects the aerodynamics, and heat transfer over the entire airfoil. The leading edge region of the airfoil has the highest heat transfer rate over the entire airfoil. Typically, coolant from within the airfoil is injected through several rows of discrete hole around the leading edge region to protect the surface and reduce the heat transfer rates. The interaction between the mainstream gases and the coolant jets varies from stagnation with increases interaction downstream on the suction and pressure surfaces.

Leading edge region of the turbine blade has been a focus for many film cooling studies. Mick and Mayle (1988), Karni and Goldstein (1990), Mehendale and Han (1992) studied the effects of free-stream turbulence, injection hole geometry, blowing ratio, coolant density on heat transfer and film cooling effectiveness for a blunt body with a circular leading edge and a flat after-body. Funazaki *et al.* (1995) presented the effect of periodic unsteady wake passing on film effectiveness for a similar leading edge model.

Recently, Ekkad *et al.* (1997) presented detailed heat transfer coefficient and film effectiveness distributions on a circular cylindrical leading edge model with two rows of film holes. They used a transient liquid crystal technique to measure the heat transfer coefficients and film effectiveness on a cylindrical leading edge film cooling model. Figure 18 shows the effect of free-stream turbulence on detailed film effectiveness distributions using CO_2 as coolant. Free-stream turbulence significantly reduces film effectiveness for blowing ratio $M = 0.4$ from $Tu = 1\%$ to 7.1%. This is because higher free-stream turbulence breaks down coolant jet structure at low blowing ratio. At higher blowing ratio $M = 1.2$, the effect of free-stream turbulence is not so significant with more uniform effectiveness over the entire surface at higher free-stream turbulence. Effectiveness downstream of the hole is reduced with an increase in free-stream turbulence.

FLAT SURFACE FILM COOLING SIMULATION

Goldstein (1971) presented a review of all film cooling literature on flat surface film cooling prior to 1971. He presented the effects of various geometrical and flow parameters affecting film cooling. Many researchers have studied film cooling on flat surfaces. Flat surface model can be used to study the effect of individual parameter easily and economically. Early studies have proved that the results obtained on simple flat surface models can be applied to real engine design with some corrections. The effects of geometrical parameters (hole geometry, shape, size), and flow parameters (coolant-to-mainstream mass flow, density ratio, mainstream Reynolds number, velocity, etc.) have been studied on flat surfaces. Eriksen and Goldstein (1974), Hay *et al.* (1985), and Ammari *et al.* (1990) studied the effects of blowing ratio, density ratio, and film hole geometries on heat transfer coefficients over a flat surface. Pedersen *et al.* (1977), Foster and Lampard (1980), and Sinha *et al.* (1991) studied the effects of density ratio on film effectiveness over a flat surface. Ligrani *et al.* (1992), Schmidt and Bogard (1996), and Ekkad *et al.* (1997a,b) presented the increased heat transfer coefficient and film effectiveness for compound angle film cooling. Bons *et al.* (1994), and Schmidt and Bogard (1996) reported the effects of high free-stream turbulence on reducing flat plate film cooling performance. Schmidt *et al.* (1996) and Gritsch *et al.* (1997, 1998) presented the improved film cooling effectiveness with the shaped film cooling holes.

Figure 19 shows the effect of compound angle injection on detailed film effectiveness distribution using a transient liquid crystal method (Ekkad *et al.*, 1997a). In general, compound angle injection ($\beta = 45°$ or $90°$) provides more coverage and effectiveness than simple angle injection ($\beta = 0°$). The lateral interaction of the jets with the mainstream

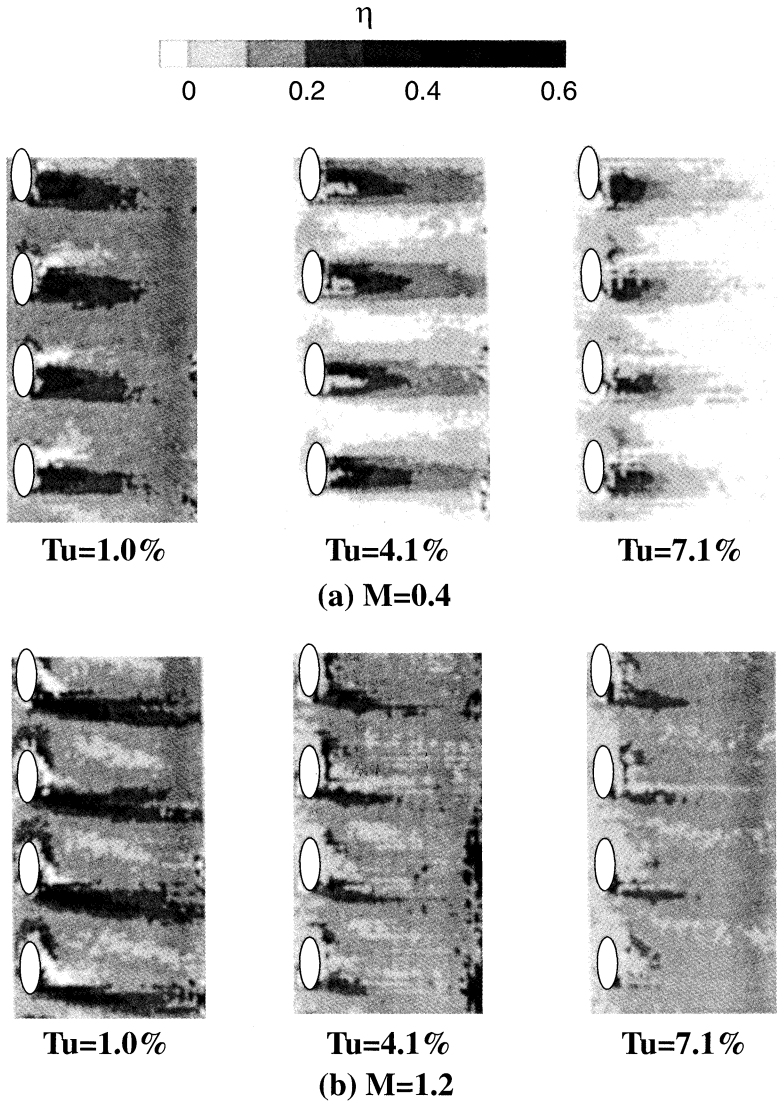

FIGURE 18 Effect of free-stream turbulence on detailed film effectiveness distributions of a cylindrical leading edge model (Ekkad *et al.*, 1997).

for compound angle injection could be attributed to the higher and more uniform effectiveness on the surface. Figure 20 shows the cylindrical fanshaped and laidback fanshaped hole used by Gritsch *et al.* (1997), and the effect of hole shape on local film effectiveness using an IR camera method. For the cylindrical hole, the jet was detached from the surface at the higher blowing ratio resulting in a poor effectiveness. For the fanshaped hole jet spreading is much better that results a better effectiveness. For the laidback fanshaped hole, jet spreading is the best that result the highest overall effectiveness, particularly at high blowing ratios.

CONCLUSIONS

Most of the existing experimental film cooling data are applicable for the main body of turbine airfoil studies. However, turbine airfoil edge cooling

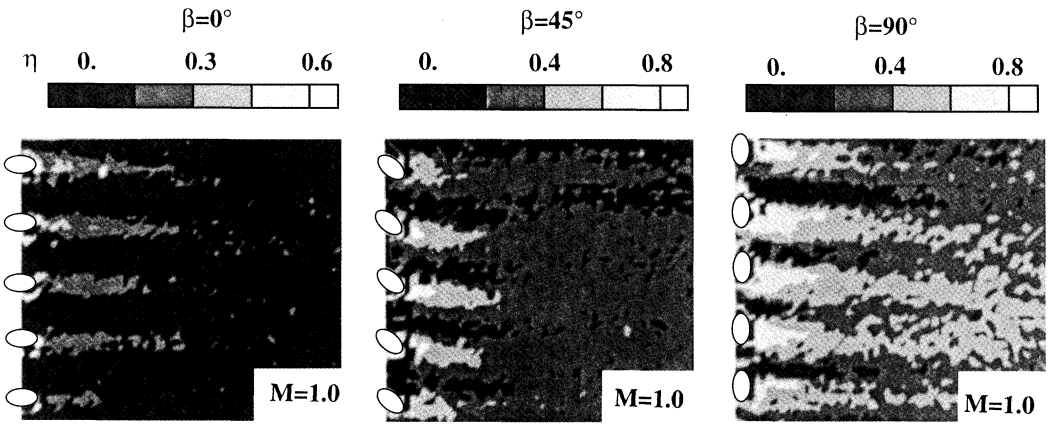

FIGURE 19 Effect of compound-angle injection on detailed film effectiveness distributions over a flat surface (Ekkad *et al.*, 1997a).

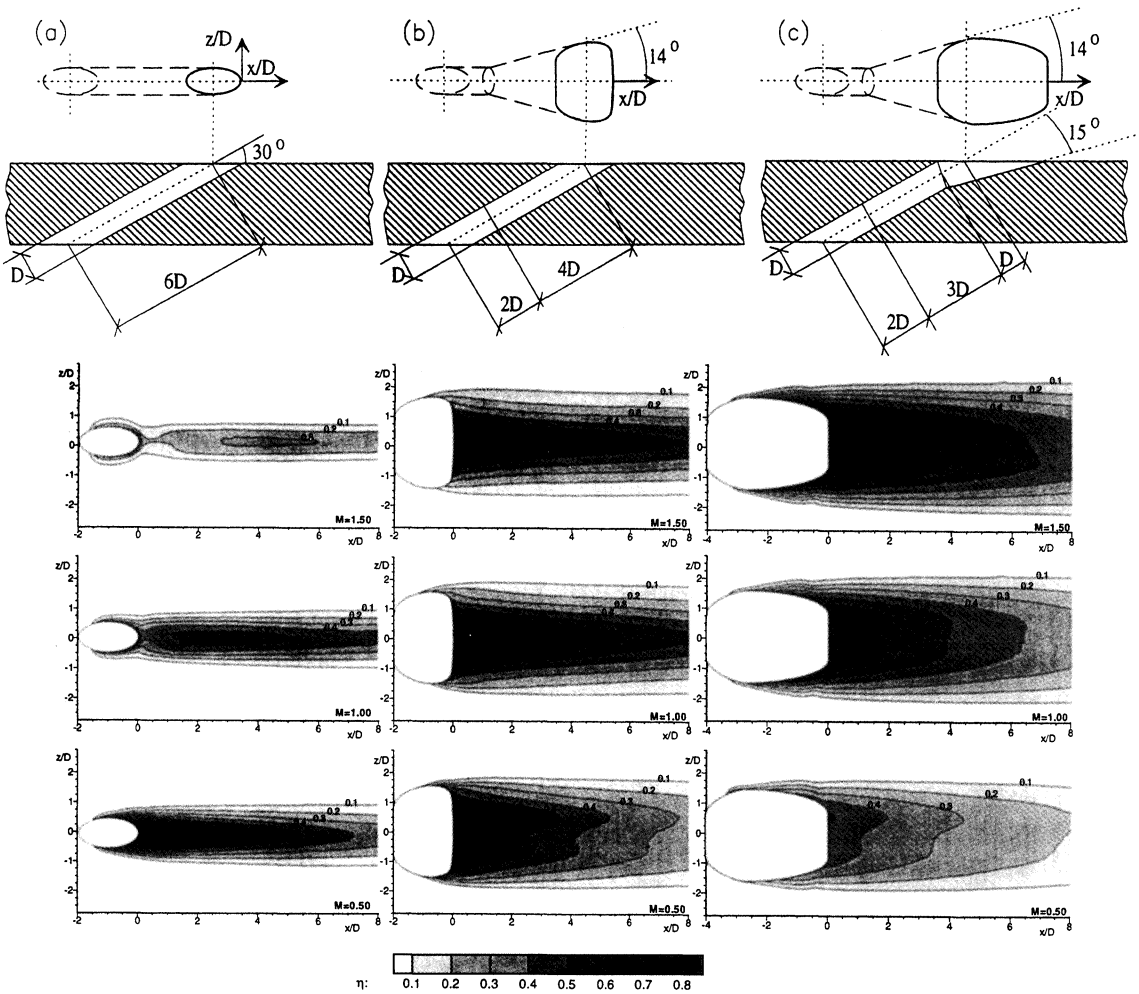

FIGURE 20 Local effectiveness η for the cylindrical, fanshaped, and laidback fanshaped hole at $Ma_m = 0.6$, $Ma_c = 0.0$, and $\beta = 0°$ (Gritsch *et al.*, 1998).

becomes an urgent issue for the next century gas turbines to satisfy the higher rotor inlet temperature requirement. Edge-cooling heat transfer includes: turbine vane endwall heat transfer and film cooling, airfoil trailing edge region film cooling heat transfer, and turbine rotor blade tip region heat transfer with and without tip hole cooling under realistic engine flow conditions. Accurate and detailed local heat transfer and film cooling data for turbine edge region would be useful to prevent blade failure due to local hot spots. Flow visualizations/measurements, and the CFD predictions would provide valuable information for designing effective cooled blades for advanced gas turbines.

References

Abhari, R.S. and Epstein, A.H. (1994), An experimental study of film cooling in a rotating transonic turbine, *ASME Journal of Turbomachinery*, **116**, 63–70.

Abuaf, N., Bunker, R. and Lee, C.P. (1995), Heat transfer and film cooling effectiveness in a linear airfoil cascade, *ASME* Paper 95-GT-3.

Ames, F.E. (1997), Aspects of vane film cooling with high turbulence Part I-Heat transfer, Part II-Adiabatic effectiveness, *ASME* Paper 97-GT-239, 97-GT-240.

Ammari, H.D., Hay, N. and Lampard, D. (1990), The effect of density ratio on the heat transfer coefficient from a film-cooled flat plate, *ASME Journal of Turbomachinery*, **112**, 444–450.

Bons, J.P., MacArthur, C.D. and Rivir, R.B. (1994), The effect of high free-stream turbulence on film cooling effectiveness, *ASME Journal of Turbomachinery*, **118**, 814–825.

Camci, C. and Arts, T. (1985a), Experimental heat transfer investigation around the film-cooled leading edge of a high-pressure gas turbine rotor blade, *ASME* Paper 85-GT-114.

Camci, C. and Arts, T. (1985b), Short-duration measurements and numerical simulation of heat transfer along the suction side of a film-cooled gas turbine blade, *ASME* Paper 85-GT-111.

Camci, C. and Arts, T. (1990), An experimental convective heat transfer investigation around a film-cooled gas turbine blade, *ASME Journal of Turbomachinery*, **112**, 497–503.

Drost, U. and Bölcs, A. (1998), Investigation of detailed film cooling effectiveness and heat transfer distributions on a gas turbine airfoil, *ASME* Paper 98-GT-20.

Du, H., Han, J.C. and Ekkad, S.V. (1997), Effect of unsteady wake on detailed heat transfer coefficient and film effectiveness distributions for a gas turbine blade, *ASME* Paper 97-GT-166.

Ekkad, S.V., Han, J.C. and Du, H. (1997), Detailed film cooling measurements on a cylindrical leading edge model: effect of free-stream turbulence and coolant density, *ASME* Paper 97-GT-181.

Ekkad, S.V., Zapata, D. and Han, J.C. (1997a), Film effectiveness over a flat surface with air and CO_2 injection through compound angle holes using a transient liquid crystal image method, *ASME Journal of Turbomachinery*, **119**, 587–593.

Ekkad, S.V., Zapata, D. and Han, J.C. (1997b), Film effectiveness over a flat surface with air and CO_2 injection through compound angle holes using a transient liquid crystal image method, *ASME Journal of Turbomachinery*, **119**, 580–586.

Eriksen, V.L. and Goldstein, R.J. (1974), Heat transfer and film cooling following injection through inclined circular tubes, *ASME Journal of Heat Transfer*, **96**, 239–245.

Foster, N.W. and Lampard, D. (1980), The flow and film cooling effectiveness following injection through a row of holes, *ASME Journal of Engineering for Power*, **102**, 584–588.

Friedrichs, S., Hodson, H.P. and Dawes, W.N. (1996), Distribution of film cooling effectiveness on a turbine endwall measured using the ammonia and diazo technique, *ASME Journal of Turbomachinery*, **118**, 613–621.

Friedrichs, S., Hodson, H.P. and Dawes, W.N. (1998), The design of an improved endwall film-cooling configuration, *ASME* Paper 98-GT-483.

Funazaki, K., Yokota, M. and Yamawaki, S. (1995), The effect of periodic wake passing on film effectiveness of discrete cooling holes around the leading edge of a blunt body, *ASME* Paper 95-GT-183.

Goldstein, R.J. and Spores, R.A. (1988), Turbulent transport on the endwall in the region between adjacent turbine blades, *ASME Journal of Turbomachinery*, **110**, 862–869.

Goldstein, R.J. (1971), Film cooling, *Advances in Heat Transfer*, **7**, 321–379.

Gritsch, M., Schulz, A. and Wittig, S. (1997), Adiabatic wall effectiveness measurements of film cooling holes with expanded exits, *ASME* Paper 97-GT-164.

Gritsch, M., Schulz, A. and Wittig, S. (1998), Heat transfer coefficient measurements of film-cooling holes with expanded exits, *ASME* Paper 98-GT-28.

Harasgama, S.P. and Burton, C.D. (1991a), Film cooling research on the endwall of a turbine nozzle guide vane in a short duration annular cascade, Part 1: Experimental techniques and results, *ASME* Paper 91-GT-252.

Harasgama, S.P. and Burton, C.D. (1991b), Film cooling research on the endwall of a turbine nozzle guide vane in a short duration annular cascade, Part 2: Analysis and correlation of results, *ASME* Paper 91-GT-253.

Hay, N., Lampard, D. and Saluja, C.L. (1985), Effects of cooling films on the heat transfer coefficient on a flat plate with zero mainstream pressure gradient. *ASME Journal of Engineering for Gas Turbines and Power*, **107**, 104–110.

Jabbari, M.Y., Marston, K.C., Eckert, E.R.G. and Goldstein, R.J. (1994), Film cooling of the gas turbine endwall by discrete-hole injection, *ASME* Paper 94-GT-67.

Karni, J. and Goldstein, R.J. (1990), Surface injection effect on mass transfer from a cylinder in crossflow: a simulation of film cooling in the leading edge region of a turbine blade, *ASME Journal of Turbomachinery*, **112**, 418–427.

Kim *et al.* (1995), A summary of the cooled turbine blade tip heat transfer and film effectiveness investigations performed by Dr. D.E. Metzger, *ASME Journal of Turbomachinery*, **117**, 1–11.

Ligrani, P.M., Ciriello, S. and Bishop, D.T. (1992), Heat transfer, adiabatic effectiveness and injectant distributions downstream of a single row and two staggered rows of compound angle film-cooled holes, *ASME Journal of Turbomachinery*, **114**, 687–700.

Mehendale, A.B. and Han, J.C. (1992), Influence of high mainstream turbulence on leading edge film cooling heat transfer, *ASME Journal of Turbomachinery*, **114**, 707–715.

Mehendale, A.B., Han, J.C., Ou, S. and Lee, C.P. (1994), Unsteady wake over a linear turbine blade cascade with air and CO_2 film injection: Part II-Effect on film effectiveness and heat transfer distributions, *ASME Journal of Turbomachinery*, **116**, 730–737.

Mick, W.J. and Mayle, R.E. (1988), Stagnation film cooling and heat transfer, including its effect within the hole pattern, *ASME Journal of Turbomachinery*, **110**, 66–72.

Nirmalan, N.V. and Hylton, L.D. (1990), An experimental study of turbine vane heat transfer with leading edge and downstream film cooling, *ASME Journal of Turbomachinery*, **112**, 477–487.

Ou, S., Han, J.C., Mehendale, A.B. and Lee, C.P. (1994), Unsteady wake over a linear turbine blade cascade with air and CO_2 film injection: Part I-Effect on heat transfer coefficients, *ASME Journal of Turbomachinery*, **116**, 721–729.

Pedersen, D.R., Eckert, E.R.G. and Goldstein, R.J. (1977), Film cooling with large density differences between the mainstream and the secondary fluid measured by the heat-mass transfer analogy, *ASME Journal of Heat Transfer*, **99**, 620–627.

Schmidt, D.L. and Bogard, D.G. (1996), Effects of Free-stream turbulence and surface roughness on film cooling, *ASME* Paper 96-GT-462.

Schmidt, D.L., Sen, B. and Bogard, D.G. (1996), Film cooling with compound angle holes: Adiabatic effectiveness, *ASME Journal of Turbomachinery*, **118**, 807–813.

Sinha, A.K., Bogard, D.G. and Crawford, M.E. (1991), Film cooling effectiveness downstream of a single row of holes with variable density ratio, *ASME Journal of Turbomachinery*, **113**, 442–449.

Takeishi, K., Aoki, S., Sato, T. and Tsukagoshi, K. (1992), Film cooling on a gas turbine rotor blade, *ASME Journal of Turbomachinery*, **114**, 828–834.

Takeishi, K., Matsuura, M., Aoki, S. and Sato, T. (1990), An experimental study of heat transfer and film cooling on low aspect ratio turbine nozzles, *ASME Journal of Turbomachinery*, **112**, 488–496.